Original Paper

Cellular Physiology and Biochemistry

Cell Physiol Biochem 2011;28:833-846

Accepted: October 07, 2011

NF-κB as Node for Signal Amplification During Weaning

Luis Torres, Eva Serna, Ana Bosch, Rosa Zaragozá, Concha García, Vicente J. Miralles, Juan Sandoval, Juan R. Viña and Elena R. García-Trevijano

Departamento de Bioquímica y Biología Molecular, Fundación Investigación Hospital Clínico Valencia/ INCLIVA, Universitat de Valencia, Valencia

Key Words

p65/p300 • Regulatory node • ChIP-on-Chip • Mammary gland • Involution Inflammation

Abstract

Post-lactational involution has been reported to share common features with breast tumor development. A deep characterization of the signaling triggered after weaning would help to unveil the complex relationship between involution and breast cancer. NF-κB, a crucial factor in the involuting gland, might be an important regulatory node for signal amplification after weaning; however there is limited information about the identity of NF-κB-target genes and the molecular mechanisms leading to the selection of genes involved in a particular biological process. We identified 4532 target genes in mammary gland at 48h weaning, by genome-wide analysis of regions bound by RelA(p65)-NF-κB *in vivo*. It was found that among total RelA(p65)-NF-κB-enriched genes, only 268 bound the trans-activating complex p65/p300. Our results suggest that the latter represents a major complex preferentially involved in the modulation of the inflammatory response at 48h of mammary gland involution. A genome-wide factor location analysis revealed that p65-binding had a heterogeneous distribution while the complex of p65 and its co-activator p300 were mainly bound to proximal promoters near transcription start sites. Moreover, our computational analysis predicts the existence of cooperating elements on RelA-NF-κB/p300-enriched genes that could explain preferential binding and modulation of gene expression during mammary gland involution.

Introduction

Coordination between different biological processes is a major issue for the understanding of tissue homeostasis and still, the molecular mechanisms explaining this control remain far unknown. In this sense, the developmental cycle of the murine mammary gland is a good example of a complex process finely tuned by different signals. Following lactation and the weaning of the pups, the mammary gland undergoes a sequential chain of events known as involution which ends up with the gland returning to a pre-pregnant like state.

KARGER

Fax +41 61 306 12 34
E-Mail karger@karger.ch
www.karger.com

1015-8987/11/0285-0833$38.00/0

Accessible online at:
www.karger.com/cpb

Juan R. Viña
Departamento de Bioquímica y Biología Molecular
Facultad de Medicina, Universidad de Valencia
Avda. Blasco Ibañez 17, E-46010 Valencia (Spain)
Tel. +34-963864187, Fax +34-963864001, E-Mail juan.R.vina@ uv.es

Mammary gland involution goes through two coordinated stages: while the first stage involves alveolar programmed cell death, the second one is characterized by lobular-alveolar remodeling of the gland and adipogenesis [1]. Each of these stages exhibit prototypical changes in gene expression and protein activity. Nonetheless, some of the regulatory signals triggered during the first onset of mammary gland involution persist throughout the whole process [2].

A deeper study into the molecular mechanisms involved in the regulation of mammary gland involution revealed different biological processes overlapping at the same time. Indeed, cell proliferation occurs not only during virgin development and pregnancy as thought at first, but also during mammary gland involution with a peak of DNA synthesis at 48h after weaning [2]. On the other hand, our group and others have described the induction of inflammatory acute phase response genes in mammary gland at 48h after pups withdrawal [3-6]. Concomitant induction of inflammatory, apoptotic and proliferative regulatory signals could represent conflicting messages for cells. However, under physiological conditions, a fine balance among these responses will condition tissue homeostasis, and therefore cell proliferation or apoptosis resolution will depend upon which side the balance is tilted.

In this sense, although the molecular mechanisms involved in the inclination to a particular biological process remain elusive, it is not unusual to find common regulatory proteins for the above mentioned processes [7- 9]. Most of these proteins have been identified as oncogenes or transcription factors persistently activated during neoplasic transformation, a circumstance which adds an increased interest for health purposes. Such is the case for transcription factor NF-κB, which plays a major role in inflammation, cell survival, proliferation and oncogenesis [10].

NF-κB comprises a family of five structurally and functionally related transcription factors. Based on their transactivation properties, NF-κB proteins are divided into two classes: Class I consist of RelA (p65), Rel B, and c-Rel and class II includes NF-κB1/p50 and NF-κB2/p52. All of them can dimerize in almost any combination but only Rel proteins posses C-terminal transactivation domain and N-terminal Rel homology domain (RHD), the latter being responsible for dimerization, nuclear translocation, DNA binding and interaction with NF-κB cytoplasmic inhibitor, IκB [11].

Among this family of transcription factors, two NF-κB subunits, RelA (p65) and p50 are expressed at different levels in the mammary epithelium throughout mammary gland development, with two major peaks of activation during pregnancy and involution [12]. In fact, overlapping with a cascade of pro-inflammatory signals, increased NF-κB activity can be detected as soon as 1h after weaning [13] and it remains activated at 3 days after removal of the pups [12]. This pattern of NF-κB activity seems to be critical for mammary gland development and involution. It has been shown that defective activation of NF-κB in IKKα knockin mice displays impaired proliferation of the lobuloalveolar tree during pregnancy [14]. More importantly, when uncoupled from its physiological mode of regulation, constitutive activation of NF-κB in c-Rel transgenic mice leads to tumor development [15]. Accordingly, mammary epithelium from IκBα knockout mice, which renders increased NF-κB activity, transplanted into wild type mice shows increased lateral ductal branching and pervasive intraductal hyperplasia [16]. Even more, clinical evidences link NF-κB activation to a prognosis marker for ER-positive primary breast cancer [17]. Nevertheless, although most reports associate NF-κB activation with survival pathways [13, 18], this transcription factor has also been shown to modulate the induction of pro-apoptotic genes. Indeed, defective NF-κB signaling in conditional IKKβ knockout mice abrogated caspase-3 activity during involution and delayed apoptosis and remodeling of the gland [19].

Consistent with these data, it has been suggested that NF-κB may play a major role as a checkpoint regulator in the mammary gland after weaning. Identification of NF-κB-regulated genes *in vivo* will help our understanding of the complex interplay between opposite signals. In the present manuscript we explore the role of NF-κB as a node of regulation in mouse mammary gland involution by ChIP-on-Chip experiments. We identified the NF-κB target genes in mouse mammary gland at 48h after weaning. Moreover, genome-wide factor location analysis with antibodies specific for mouse p65 subunit and its coactivator p300 showed that only 268 genes, out of the 4532 initially found to bind p65, bound NF-κB as a p65/p300 transactivating complex. Finally, in this manuscript we studied the molecular functions and common features of genes regulated by RelA(p65)/NF-κB and analyzed putative co-operating transcription factors that could explain preference binding and modulation of gene expression during mammary gland involution.

Material and Methods

Reagents

General reagents were purchased from Sigma Chemical Co. (St Louis, MO) Antibodies against α-(p65)NF-κB and RNApol II were from SantaCruz Biotechnology (Santa Cruz, CA). Antibodies α-p300, were from Cell Signaling. Reagents for qPCR were from Applied Biosystems (Foster city, CA).

Animals

Female mice (C57BL6) were from Taconic. Animals were kept in individual cages in a controlled environment (12h dark/12h light cycle) and received water and food *ad libitum*. The studies satisfied the guidelines for humane treatment of animals and were approved by the Research Committee of the School of Medicine at the University of Valencia. The mice were handled in agreement with the National Institutes of Health guidelines and the Guiding Principles for Research Involving Animals and Humans approved by the Council of the American Physiological Society.

Following parturition, litters were maintained with at least seven pups. At the peak of lactation (days 9-11) mice were separated into two groups: a control group of lactating mice and a weaned group whose pups were removed 48h before sacrifice. Mice were given a single dose of i.p. sodium pentobarbital (60mg/kg of body weight). Inguinal mammary glands were removed and tissue samples from each experimental condition were formaldehyde-crosslinked or snap frozen in liquid nitrogen and stored at -80°C for future analysis.

ChIP assay

Formaldehyde-fixed tissue samples were immunoprecipitated according to Torres et al. [20]. Briefly, 0.5 gr. of fixed-inguinal mammary tissue were homogenized and chromatin extracted as described. Crosslinked chromatin was subjected to sonication with a Vibra-Cell VCX-500 sonicator. The diluted chromatin was pre-cleared and supernatants incubated with 2 µg of the corresponding antibody at 4°C overnight. Immunocomplexes were incubated with blocked protein A/G-sepharose for an additional period of 4h and recovered as previously described. An aliquot of crosslinked-chromatin was subjected to the same immunoprecipitation reaction in the presence of normal serum IgG and used as negative control (NS). An aliquot of whole chromatin was collected and labeled as input.

ChIP-on-ChIP

Amplification and labelling. The products of three independent ChIP assays were amplified, labeled and hybridized to mouse promoter 1.0 Array (Affymetrix UK. Ltd., High Wycombe, UK). Briefly, immunoprecipitated and input DNA were purified and amplified by ligation-mediated PCR. DNA was blunt-ended by T4 DNA polymerase and then ligated with pre-designed linkers using a T4 DNA ligase. The ligation-mediated PCR was performed as described elsewhere. PCR-amplified ChIP targets were purified with Affymetrix cDNA cleanup columns, provided in the Genechip Sample Cleanup Module. Amplified DNA (1 µg) was used for the fragmentation reaction and labeling using the Affymetrix GeneChip WT Double-Stranded DNA Terminal Labeling Kit protocol

Microarray hybridization. Arrays hybridization was performed according to the Affymetrix-recommended protocol. In brief, after a 16 h hybridization (45°C), the hybridization cocktail was removed, and the arrays were washed and stained in an Affymetrix GeneChip fluidics station 450. Arrays were scanned on an Affymetrix GeneChip Scanner 3000 7G (Affymetrix, Santa Clara, CA, USA). GeneChip Operating Software supplied by Affymetrix was used to generate CEL files.

Quality control of microarray data (3 p65 arrays, 3 p300 arrays and 3 input DNA arrays) was performed using Affymetrix Tiling Analysis Software and R/Bioconductor. Plotted histograms of the raw data intensity suggested that enrichment by both p65 and p300 was optimal in all the experiments performed.

Data analysis. The automated Genomatix ChipInspector package was used in order to determine the NF-κB and its coactivator p300 binding sites on mouse promoters regions during weaning. CEL. files were imported into ChipInspector, for linear total intensity normalization and Log2 transformation. The procedure combines one-class statistical analysis (Input *vs*. Bound) with exhaustive matching and six different experiments (comparisons). A single *t*-test related to the significance analysis of microarrays algorithm [21] was performed at the single probe level. A minimum of three consecutive probes in a window size of 300 bp was used as standard settings based on our experience with Affymetrix GeneChip Mouse Promoter Array. As indicated by software manufacturers, probes with scores higher than a certain threshold are considered significant. For each Delta value or threshold there is a relation of significant probes to falsely discovered probes, being this relation or False Discovery Rate (FDR), a stringency indicator. In order to diminish the possibility of including falsely detected probes we selected a high stringent Delta value so that we obtained a FDR of 0% for both, p65 and its coactivator p300. Although this approach decreased the number of detected probes, the danger to get falsely discovery probes was dramatically reduced compared to higher FDR values typically used in most papers. This analysis resulted in 15879 significant positive probes for p65 and 61918 for p300 (weblink to graphic output of the ChipInspector statistical calculation http://www.uv.es/eruizy/).

Promoter analysis. The p65, p300 or p65/p300-enriched regions from ChipInspector analysis were directly subjected to downstream sequence analysis using the RegionMiner tool (Genomatix). RegionMiner displays the location of proximal gene loci promoter region and transcription start sites.

The program GePS (Genomatix), which combines literature analysis with genome annotation, was used to create a subgroup of ChIP-chip enriched genes included into programmed cell death/survival, inflammation or cell proliferation categories. Groups were clustered according to co-citation and presence of NF-κB binding sites in the proximal promoter regions. Sequences spanning 500 bp upstream of the

gene	P65/p300 ChIP assay primers (5'-3')		RNApol II ChIP assay primers (5'-3')	
	Forward primer	Reverse primer	Forward primer	Reverse primer
arntl	agaaatccacagagcgtgcc	ctactttccgaccaatccgc		
canx	aaatcaggaaacagcacggg	ttccgacccattgagttagg		
capn1	taccgtttgtctagcgtccg	ggggtatttttaactagggcc	tagtgttgagagtcacaccc	actgaaggatttgggaagcg
capn2	agatggacacaccagtagcc	acgacaatcgcaagttggg	ctaggacagaactcaaaggg	cgtttcatagtcagacctcc
ccnd3	tgtgcctcagtatcatggtc	tggaatgctcctacgtcaca		
creb1	taaaactccagcgagatccg	ccgccattattctttgttcgc		
ctsl	gttatgcaactctccaccct	ctcaggctttaaagcctctc	tgactcctgtgaagaaccag	gagatcctgtctcattcagg
e2f3	aggagagacttggaaactcc	tgaggatctggatgtacgtg		
e2f5	aaagagctgggggtctactt	ccgagtttaaatggcaggaag		
flna	gctgagttgcttttggcgga	gagagctcattttgaggc	gcactattccatctcaatgcc	cttcactttaaccaagcaccc
foxo3	aaaagacgggagttgcccgcg	ggagacgcgagcgaatcgac		
htra2	ttaccggtgcgagtcaaagag	atgccgggaaacgtagtccc		
mbp	ttgtgtccaaagaagcagcg	agaggtctaaatggcatcgc	atccagaacaatgggacctc	tccatggtacttgctgtggc
mpo	cagcgaatgacaagtatcgc	catcttcatactctgcaggc	tgatagtgccaaaaggaggg	cttgaagcagttttgcccag
Pias1	aaatagtgcgtgtgggtctc	ctacaactccagactcgggt		
rarg	atccttggaaacccactgga	tcagcatctcaaatggtggc	atccttggaaacccactgga	tcagcatctcaaatggtggc
ripk1	agtagtccttagaggaggac	agcttctgaggaaactagcg		
runx3	acttctttctgccacagacc	taatttcaggatcgcgcagg	cctcagcagtaaacagagag	tgcagatctggagtgagcgga
stat5b	ggctactatggacttctgcc	cgcttcctggttcctgcc		
tle1	cgcgtgttaatgtaagcgg	ttagcaaagggctgaccag		
trp73	aacactctgcagtgccactaa	gactcttcaaagtccagcca	gctcctgtaacaagacacc	tagtcggtattggaaggga
uchl1	ggtgcccattatttgtctgg	cacaacactgcgtatccact	aaggatcccacttcttaggg	ttgacttaagcaagccaggc
cmyc	gggtacatggcgtattgtgt	agacccccggaatataaagg		

Table 1. PCR Primer sequences for ChIp assay and RNApol II ChIP

first transcriptional start site (TSS) and 100bp downstream of the last TSS were extracted using the Gene2promoter module of Genomatix Software Suite.

Validation of selected p65/p300-bound genes by ChIP assay and PCR

DNA from Input, immunoprecipitated and NS fractions was purified with a PCR purification kit (Qiagen, Hilden, Germany) and analyzed by PCR with specific primers for selected genes. Primers were designed to render a product of 250-400 bp in length flanking that region matched by probes in the Affymetrix GeneChip Mouse Promoter Array. PCR fragments were size-fractionated by 2% agarose gel electrophoresis and stained with ethidium bromide. Primers for PCR analysis are included in Table 1. Fold enrichment for p65 or p300 on c-myc promoter by qPCR was calculated as $2^{(C_t \text{ input} - C_t \text{ IP})}$. Data was normalized by results obtained on skeletal α-actin promoter previously used as negative control for NF-κB enrichment in mammary gland after weaning [3].

RNA isolation and qPCR

Total RNA was extracted using TRIzol® reagent (Invitrogen Life Technologies) followed by additional column purification (RNeasy, Qiagen). The concentration and purity of RNA were assessed using a NanoDrop™ ND-2000 spectrophotometer (Nanodrop Technologies, DE, USA). RNA integrity was assessed using the RNA 6000 Nano LabChip Series II Assay with the 2100 Bioanalyzer System (Agilent Technologies, Palo Alto, CA, USA)

RNA (5 µg) was reverse-transcribed using the High Capacity RNA-to-cDNA kit (Applied Biosystems, Foster City, CA) and the cDNA products amplified by qPCR (Real time quantitative PCR) using the TaqMan Universal PCR Master Mix (Applied Biosystems). qPCR reactions were carried out with 1 µL cDNA in a final volume of 10 µL, using a 7900HT Fast Real-Time PCR system (Applied Biosystems). Specific primers (predeveloped Taqman primers) for c-myc and 18S (Rn00561507_m1, and Mm004878003_m1, respectively) were purchased from Applied Biosystems. Results were normalized

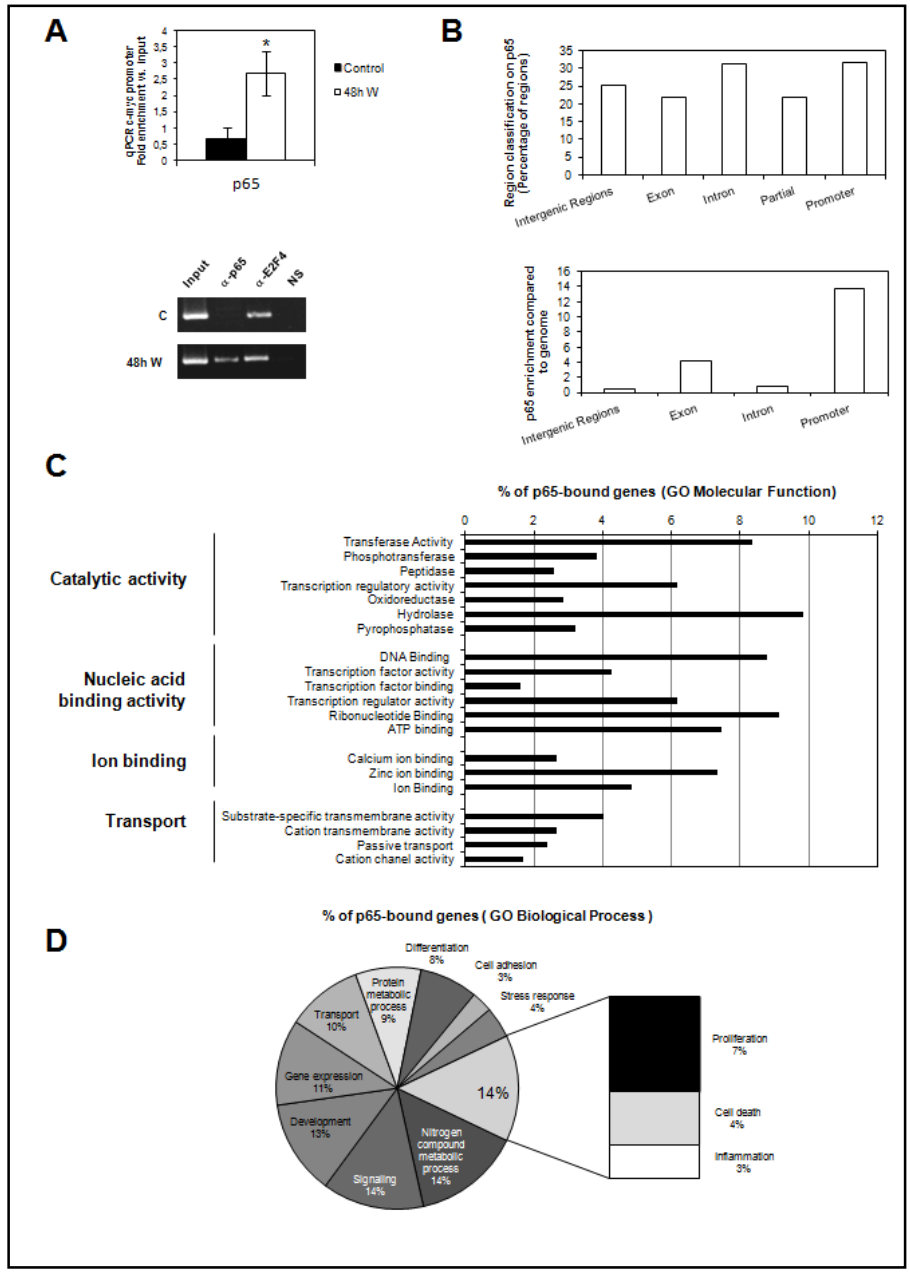

Fig. 1. Identification and characterization of RelA/NF-κB targets in mouse mammary gland at 48h weaning. (A) Validation of p65 antibody for ChIP-on-Chip analysis. p65 binding to c-myc promoter was analyzed by ChIP assay in mammary gland samples from both lactating controls and at 48h weaning using specific antibodies for p65. Anti- E2F4 antibodies or normal serum IgG were used as positive and negative controls, respectively. qPCR (upper panel) or semiquantitative PCR (lower panel) was performed using primers specific for c-myc promoter. IP signal in qPCR was defined as described in the Material and Methods section and is represented as fold enrichment in either control (black bars) or 48h weaning (white bars). The average of three independent experiments is shown (mean ± SE *P < 0.05 vs. inputs). (B) General annotation and statistics for genomic region distribution of p65. Region classification on p65 by RegionMiner tool was represented as percentage in genome (upper) and enrichment compared to genome (lower). A total of 7195 regions derived from ChipInspector analysis of p65 ChIP-on-Chip were classified. (C) Distribution of GO molecular function for p65 targets. In some instances, a gene is assigned to more than one category. Clusters are represented as percentage of p65-enriched genes included in a molecular category in relation to the total number of genes with a GO annotation. (D) Distribution of GO Biological process for p65 targets. Percentages were calculated as described above.

according to 18S quantification in the same sample reaction.

A 96-well plate was custom designed and ordered from Applied Biosystems, containing Gene Expression Assays capable of measuring mRNA for 22 NF-κB-target genes and four endogenous controls (TaqMan® Gene Expression assay preconfigured in a 96-well format, Part no. 4413260, Applied Biosystems). Each plate was customized with three identical gene sets to facilitate the analysis of three replicates per gene and per sample. Thermal cycler conditions were as follows: 2 min incubation at 50°C, 10 min at 95°C followed by 40 cycles of 95°C for 15 seconds and 60°C for 60 seconds. The relative quantity of mRNA expression was calculated using the comparative Ct ($2^{-\Delta\Delta C_t}$) method where the geometric mean of the Ct value of the endogenous control genes was used to normalize the data.

Statistical analysis

Data are the means ± SE of at least three independent experiments. Representative blots and ChIPs are shown. Statistical significance was estimated with one-sample Student's *t* test. A *p* value of less than 0.05 was considered significant.

Results and Discussion

Identification of RelA/NF-κB binding sites in mouse mammary gland involution by ChIP-on-Chip analysis

We combined chromatin immunoprecipitation and mouse whole genome promoter array profiling to identify

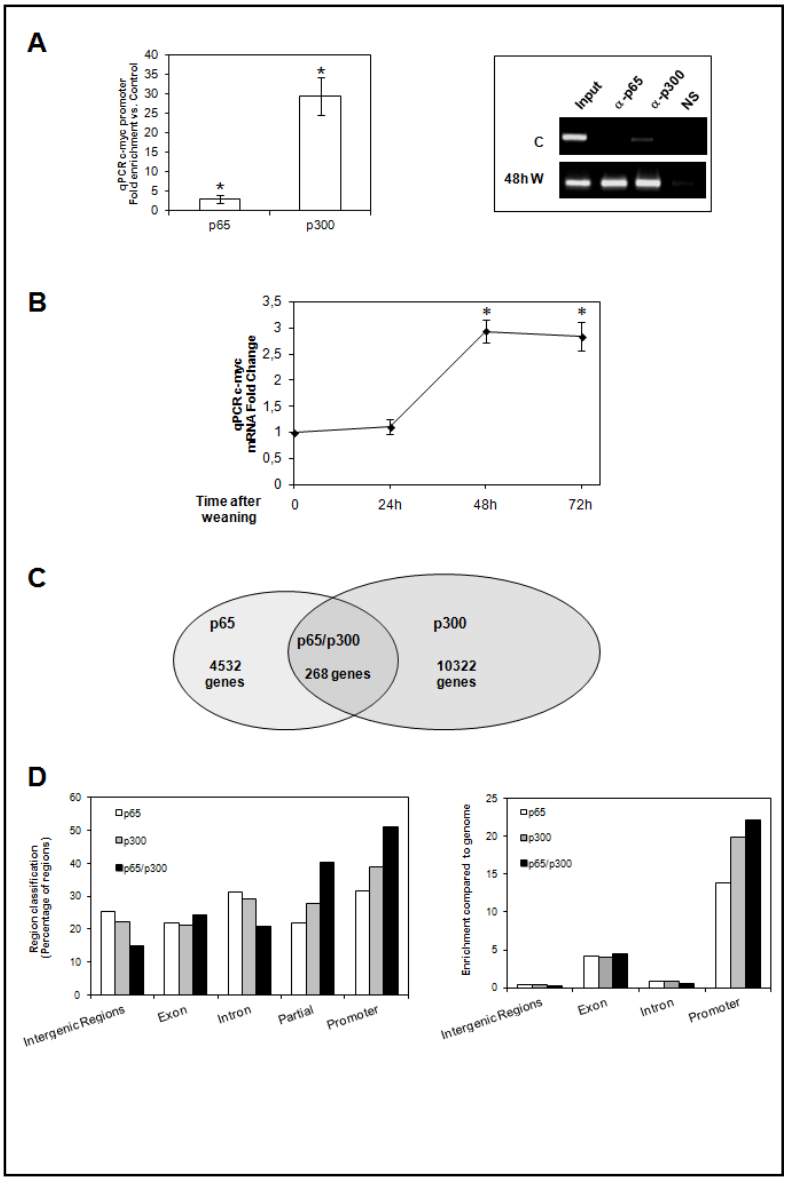

Fig. 2. ChIP-on-Chip identification of RelA(p65)NF-κB/p300-target genes in mammary gland involution. (A) Validation of p300 antibody for ChIP-on-Chip analysis. p300 binding to c-myc promoter was analyzed by ChIP assay in mammary gland samples, from both lactating (controls) and 48h weaned mice, using specific antibodies for p300. Anti- p65 antibodies or normal serum IgG were used as positive and negative controls, respectively. qPCR (left panel) or semiquantitative PCR (right panel) were performed using primers specific for c-myc promoter. IP signal in qPCR was defined as described in the Material and Methods section. Fold enrichment of p65 and p300 during weaning versus lactating control is represented, and calculated following the relation of normalized data from Weaning/Control. Data (n= 3) are mean ± SE *P < 0.05 vs. controls. (B) Total RNA from mammary tissue samples was extracted and relative c-myc expression was analyzed by quantitative Real-Time PCR at the indicated time points after weaning. All data were normalized according to 18S and quantified in the same sample reaction. Expression levels are displayed as fold increase relative to lactating controls. Data (n= 4) are mean ± SE *P < 0.05 vs. controls. (C) Venn diagrams showing overlap between p65 and p300 target genes identified in mouse mammary gland at 48h after weaning using ChIP-on-Chip. Target genes were obtained as the result of three independent experiments for each antibody. (D) General annotation and statistics for genomic region distribution of p65, p300 and p65/p300. Region classification by RegionMiner tool was compared for p65 (white bars), p300 (grey bars) and p65/p300 (black bars) and represented as percentage in genome (left panel) and enrichment compared to genome (right panel) A total of 20,000 and 947 regions derived from ChipInspector analysis of ChIP-on-Chip for p300 and p65/p300 respectively were classified.

the direct downstream targets of RelA (p65) in mammary gland at 48h involution. To validate chromatin enrichment by p65 antibody, we first analyzed by ChIP assay p65 binding to c-myc promoter, a well known NF-κB-target gene [22, 23], in tissue samples from mouse mammary gland at 48h after pups withdrawal. As positive control we used E2F4 antibody, a transcription factor known to be bound to c-myc promoter [20]. As shown in Fig. 1A, the promoter region of c-myc was two-fold enriched by p65 in samples from 48h weaning versus control lactating glands. Positive E2F4-binding and the absence of amplification in samples immunoprecipitated with normal serum IgG (Fig. 1A, lower panel) confirmed chromatin enrichment by ChIP assay.

We performed genome-wide ChIP-on-Chip experiments with Affymetrix promoter arrays that contained approximately 28,000 known mouse genes centered on the region from -6 kb to +2.5 kb relative to the TSS at an average resolution of 35 bp. Analysis of at least three independent experiments in mammary tissue samples at 48h weaning identified 4532 target genes for p65 (Weblink to RegionMiner extracted p65 raw data http://www.uv.es/eruizy/).

A genome-wide factor location analysis (Fig. 1B) revealed that positive probes for p65-binding had a heterogeneous distribution. These data are in agreement with recent evidence showing transcription factor binding to non-canonical genomic regions localized in distal

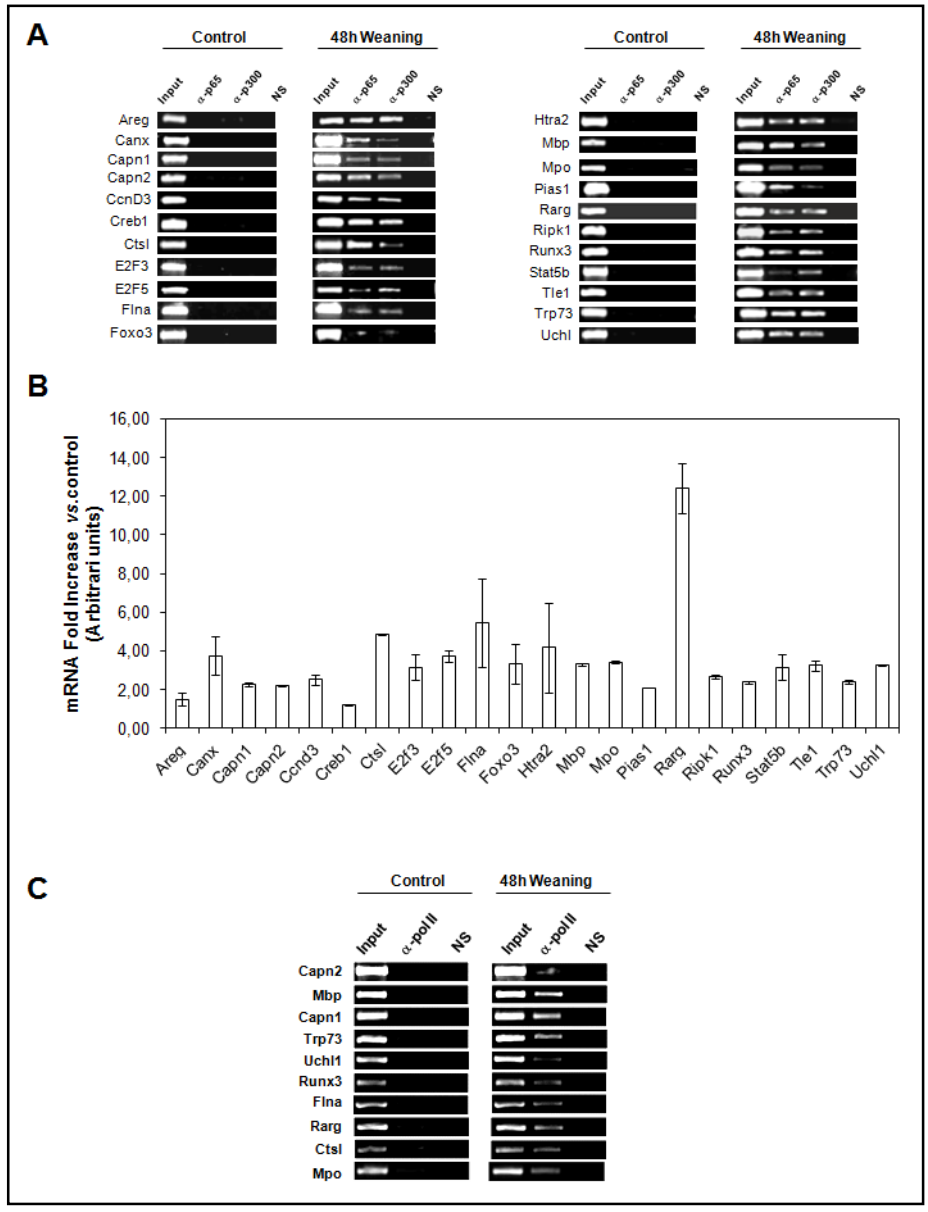

Fig. 3. Validation and gene expression analysis of p65/p300-enriched target genes. (A) Independent ChIP assays for verification of p65 and p300 occupancy on a selection of 22 target promoters during mammary gland involution. Chromatin from mammary tissue was inmunoprecipitated with antibodies against p65, p300 or normal serum IgG. Inmunocomplexes were analyzed in both lactating control and 48h weaning by semiquantitative PCR with primers specific for the selected genes. A representative experiment is shown (n=3). Primers sequence is shown in Table 1. (B) Gene expression analysis of selected p65/p300-target genes by real-time RT-PCR as described in Material and Methods section. All data were normalized and quantified in the same sample reaction. Expression levels are displayed as fold increase relative to lactating controls. Data (n = 4) are mean ± SE. Statistical difference was observed for all the analyzed genes ($P < 0.05$ *vs*. control). (C) Analysis of current transcription of selected p65/p300-target genes by RNApol II-ChIP. The presence of RNApol II on coding regions from selected genes was assessed by ChIP assay using antibodies either for RNApol II or normal serum IgG (NS). PCR was performed using specific primers for selected genes coding region (Table 1). A representative analysis (n=3) is shown.

regions from the genes they regulate [24]. Nevertheless, when p65 enrichment was compared to whole genome, a clear p65 distribution was mainly assigned to gene promoters (Fig. 1B, lower panel).

Finally, to functionally annotate our set of p65 target genes we clustered them using the Gene Ontology (GO) program GePS (Genomatix) and extensive manual curation. The percentages shown in Fig. 1C and 1D refer to the number of bound genes within a particular category in relation to the total number of bound genes that have a GO annotation. Generally, p65 target genes were enriched in categories related to molecular functions included into catalytic activity, nucleic acid binding activity, ion binding and transport (Fig. 1C). On the other hand, p65-bound genes were strongly enriched in several biological function categories (Fig. 1D), particularly in those related to nitrogen compound metabolic processes, cell signaling, development and gene expression. These results further confirm the important role played by NF-κB in mammary gland. Actually, our group has extensively studied the nitrogen compound metabolic processes that take place in mammary gland after weaning as well as the molecular consequences derived from that particular modulation [4, 25]. In this sense, we have already described the role of NF-κB on the modulation of iNOS expression during mammary gland involution [3]. The role played by NF-κB in other biological processes such as cell signaling or gene expression modulation has been exhaustively documented [12-16]. For our purposes and taking into account that sometimes a gene can be assigned to more

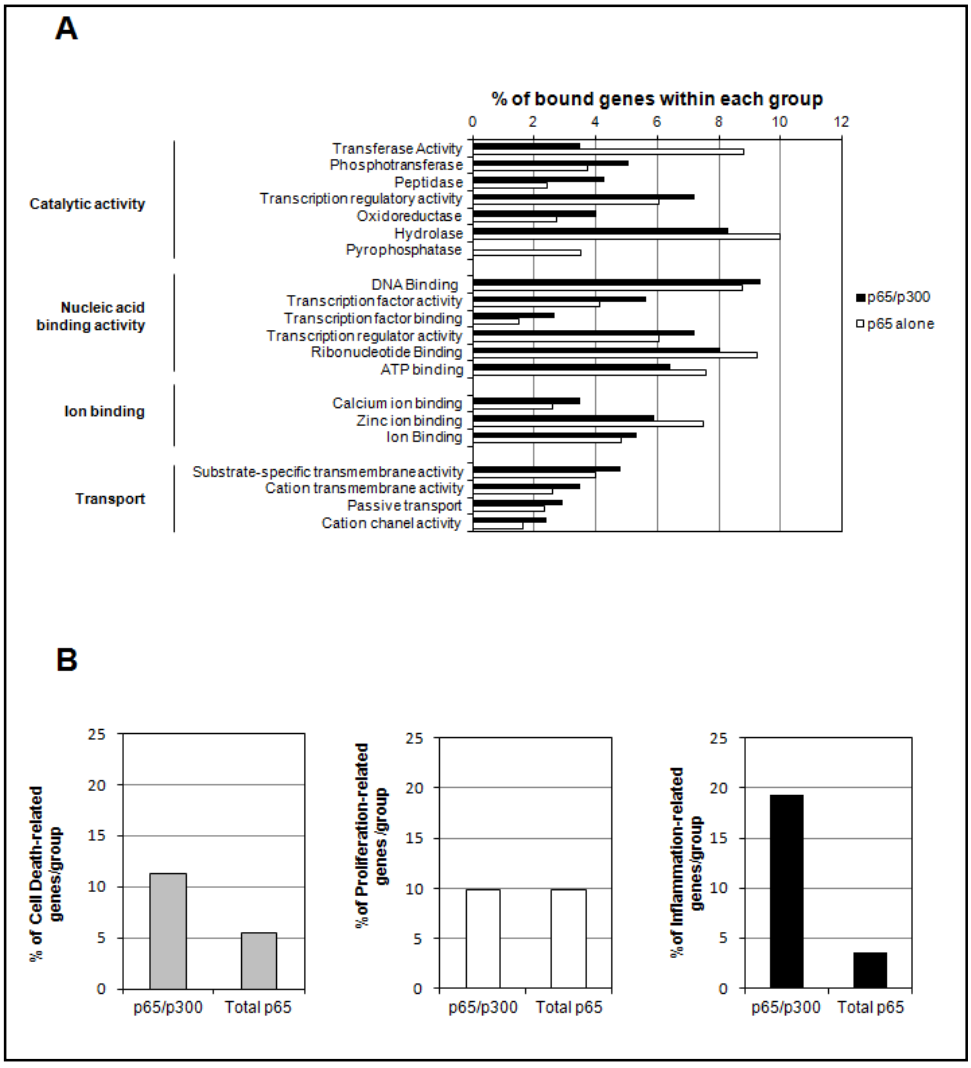

Fig. 4. Molecular and biological characterization of p65/p300-target genes. (A) Histograms depict the distribution of GO annotations clustered into molecular functions among genes bound by p65 and p300 versus total genes bound by p65. Percentages were calculated as number of bound genes within a category referred to total number of bound genes with a GO annotation. (B) The percentage of genes bound by p65, related to cell death (grey bars), proliferation (white bars) or inflammation (black bars) that fall into the indicated groups is shown. Percentages of genes were calculated as the number of genes included in a biological process *vs*. total number of genes for that category in the indicated group. *P*-values for p65/p300 group were $1.57 \cdot 10^{-8}$ (cell death), $3.60 \cdot 10^{-7}$ (proliferation) and $3.79 \cdot 10^{-8}$(inflammation).

than one category, it is noteworthy to mention that 14% of p65-target genes were included in either proliferation, cell death or inflammatory processes with a higher percentage of genes included in the cell proliferation category.

ChIP-on-Chip analysis of transcriptionally-driven NF-κB-target genes

Binding of p65 to target-gene promoters does not necessarily mean transcriptionally active NF-κB-regulated genes. In fact, it has been described that NF-κB binds to distal elements in accessible gene promoters in a silent state [26]. It is well known that canonical RelA(p65)/NF-κB transcriptional activity depends on its association to CBP/p300 [27]. Upon stimulation, p65 recruits its coactivator CBP/p300 which induces histone acetylation, a fact that ultimately will lead to gene transcription. Therefore, in order to select NF-κB transcriptionally-driven genes we performed ChIP-on-Chip experiments with antibodies specific for mouse p300 and p65.

Chromatin enrichment for p300 antibody was validated by ChIP assay with primers for c-myc promoter as described previously for p65 (Fig. 2A). Moreover, to validate a transcriptionally-active gene selection we analyzed c-myc expression by qPCR in mammary gland at 48h weaning. As shown in Fig. 2B, c-myc expression dramatically increased at 48h after weaning. These results suggest that chromatin immunoprecipitation with p65 and p300 antibodies selects transcriptionally active genes.

Data from ChIP-on-Chip experiments with p300 antibody were crossed with data obtained from ChIP-on-Chip experiments with p65 antibody. Analysis of at least three independent experiments for each factor identified 10322 target genes for p300 (Weblink to RegionMiner extracted p300 raw data http://www.uv.es/eruizy/), and 268 target genes for both, p65 and p300 (Weblink to RegionMiner extracted p65p300 raw data

http://www.uv.es/eruizy/).

Therefore, the comparison of p65 and p300 target genes indicated a limited overlap (Fig. 2C) which most likely represents the current transcriptionally-driven NF-κB-target genes. On the other hand, as expected, p300 by itself was bound to a high number of genes not related to NF-κB. In fact, p300 is a well-known coactivator of great variety of transcription factors such as CREB, STAT3, AP-1, etc [28].

We wanted to study why, among all the putative NF-κB-modulated genes, only a reduced number of genes were in fact NF-κB transcriptionally-driven genes. Therefore, we tested whether p65/p300 (which most likely represents active NF-κB) preferentially binds to a particular region when compared to genes bound by p65 (which is supposed to represent NF-κB with silent transactivation activity). A genome-wide factor location analysis (Fig. 2D, left panel) revealed a higher percentage of regions included in gene promoters that were bound by p65/p300 (51%) compared to those bound by p65 (31%). Interestingly, it seems that a higher percentage of p65-bound regions were included into intronic sequences when compared to the p65/p300-bound region classification (Fig. 2D, right panel). Nevertheless, since the global distribution of bound-regions in the genome follows the same pattern for either p65/p300 or total p65, we cannot conclude that transcriptionally active NF-κB preferentially binds to a particular region in the genome.

Validation of ChIP-on-Chip data and role of NF-κB as a major node for regulation of gene expression in mammary gland involution

We analyzed our set of genes in an exhaustive manner attending to different filters for anatomical and tissue distribution, cellular component, biological process, molecular function, diseases and chemical and drugs as well. For validation of ChIP-on-Chip data we selected the most representative group of genes according to both, the relevance of genes within an individual filter and the presence of a particular gene in all the filters tested. As a result of such analysis, the presence of p65/p300 was analyzed by ChIP assay in a selected group of 22 genes. As shown in Fig. 3A, whereas p65 and p300 were absent from all the tested gene promoters in mammary gland at the peak of lactation (control), these factors were recruited to all the selected gene promoters at 48h after pups withdrawal. Therefore, our validation analysis confirms the specificity of ChIP-on-chip data.

We analyzed the final impact of NF-κB-regulated gene transcription on the steady state mRNA levels by

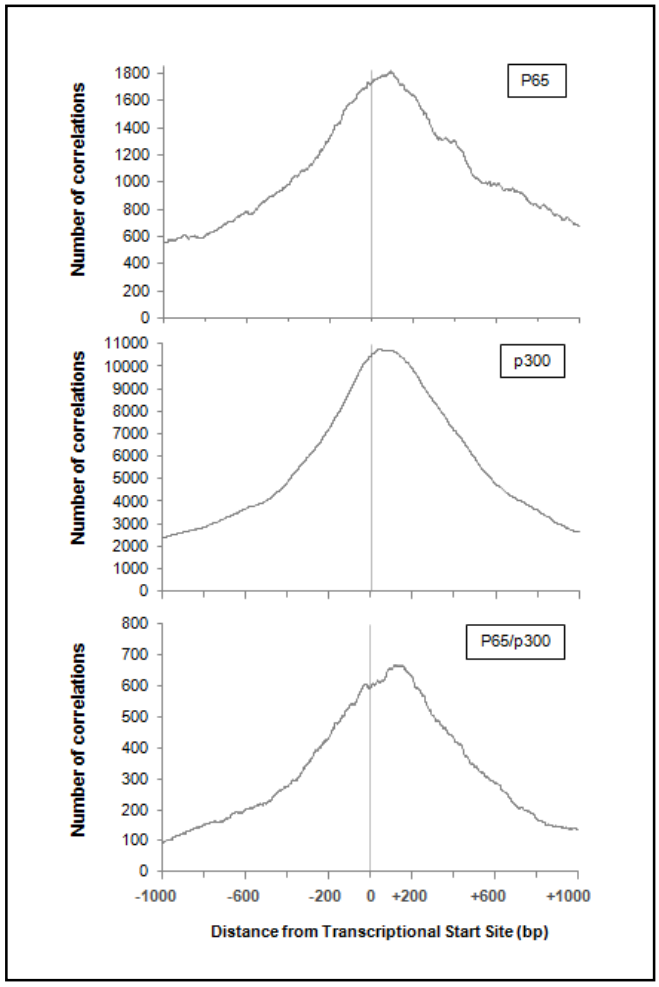

Fig. 5. Location of p65/p300 positive probes relative to TSS within a maximal distance of -1000bp to +1000bp. Transcriptional start sites involved in a correlation were plotted for p65, p300 or both p65/p300 overlapping. GenomeInspector analysis retrieved data for total p65 mean of correlations (1075±377) and most frequent distance (+93); p300 mean of correlations (5691±2687) and most frequent distance (+47); p65/p300 mean of correlations (328±175) and most frequent distance (+139).

real-time PCR in our group of 22 selected genes. As shown in Fig. 3B all the representative genes analyzed were up-regulated after 48h weaning. Data presented so far are supposed to represent a selection of NF-κB transcriptionally-driven genes within a pool of NF-κB-target genes. Nevertheless, mRNA abundance is the result of the dynamic regulation of gene transcription and mRNA stability.

The presence of RNApol II at the coding region of the gene has been shown to represent the current transcription of the gene [29].Thus, we analyzed the presence of RNApol II at the coding regions of some representative genes in mammary gland samples from

		Number of predicted V$NF-κB-binding sites										
		1		2		3		4		5		>5	
	p-value	% seq.	Ratio	% seq.	Ratio	% seq.	Ratio	% seq.	Ratio	% seq.	Ratio	% seq.	Ratio
p65/p300 enriched genes	1.29E-20	54.5	7.1E-02	19.7	4.5E-02	13.6	2.2E-02	4.5	1.1E-02	6.06	1.5E-02	1.5	3.7E-03
p65 alone enriched genes	2.43E-90	46.5	2.0E-02	30.6	1.5E-02	13.9	8.2E-03	4.3	3.1E-03	3.32	2.4E-03	1.3	9.4E-04

Table 2. Frecuency of predicted V$NF-κB-binding sites in gene promoters related to inflammation. Gene2Promoter program was used to search for V$NF-κB motifs. Input genes were those related to the inflammatory process from both p65-alone and p65/p300 enriched genes. V$NF-κB binding sites were found to be common to 86% of sequences. Frequency is expressed as percentage of sequences with the indicated number of predicted V$NF-κB- binding sites within 500bp upstream from the first TSS and 100bp downstream from the last TSS in proximal promoters. Sometimes the same gene with several TSS can be included into the 1, 2, 3, 4, 5 or >5 binding sites sub-groups. Ratio represents the number of genes with the indicated V$NF-κB -binding sites for the inflammation group versus total number of genes bound by either p65 alone or p65/p300. Raw data Weblink common TF-binding http://www.uv.es/eruizy/

both, control and 48h involution. As illustrated in Fig. 3C, RNApol II was bound to the coding regions of all tested genes, indicating a transcriptional up-regulation of these genes. These results suggest that transcriptional regulation of these genes is the main checkpoint for the observed increase of mRNA steady state levels in mammary gland after weaning.

Nevertheless, we do not rule out a possible inhibition of p65/p300 activity and repression of some NF-κB-target genes. This could be the case of parathyroid hormone-like peptide, known to be down-regulated in mammary gland after weaning and found to be a p65/p300-enriched gene.

In this sense, it has been published that low glucocorticoid concentrations (known to occur during the first stage of mammary gland involution), are able to repress NF-κB-inducible genes via direct inhibition of HAT-associated activity [30]. Finally, it has been recently described that although most of protein-coding genes experience transcriptional initiation in response to a stimulus, a subset of genes mostly encoding developmental regulators do not complete transcription [31]. In this sense, our data might suggest that transcription initiation most probably occurs at all the p65/p300 bound genes and while some genes undergo transcription elongation and mRNA processing, another fraction does not produce mature mRNAs.

All in all, although we do not exclude the relevance of other molecular mechanisms leading to the expression of a subset of genes during mammary gland involution, our experiments further support the notion of NF-κB as a major node of regulation and as a key protein involved in the amplification of the response triggered after pups withdrawal.

Role of NF-κB in the coordination of different biological processes during mammary gland involution

In order to determine the role of NF-κB as a major node of regulation at 48h of mammary gland involution, we annotate our set of p65/p300 target genes using the GePS program (Genomatix). As shown in Fig. 4A, when compared to genes bound by p65 alone (those genes that do not bind p300), p65/p300 targets were more strongly enriched in several molecular function categories, particularly those related to phosphatase, peptidase and oxidoreductase activities, transcription regulatory activity, calcium ion binding and transport. This profile is in agreement with previously published data showing a high degree of oxidative stress, an active Ca^{2+} metabolism and an increased protease activity during mammary gland remodeling [2, 3, 25]. More importantly, NF-κB regulates the expression of other transcription factors, fact that further supports its important role as a molecular platform for amplification of the involution response.

As mentioned above, the signaling pathways triggered in response to an inflammatory, apoptotic or proliferative stimulus frequently share key proteins. The confluence and synergism between common and more specific signals will ultimately favor a particular biological process above others. We propose here that NF-κB could play a role as a key protein involved in the coordination of confluent signals. If so, does NF-κB preferentially bind to genes included into a specific biological category? We

P65-bound genes		P65/p300-bound genes	
Matrix Family	p-value	Matrix Family	p-value
V$KLFS	5.4E-6	V$ETSF	0.004
V$RXRF	2.48E -5	V$KLFS	0.013
V$HAND	0.016		
V$ETSF	0.05		

P65-bound genes with predicted V$NF-κB binding sites		P65/p300-bound genes with predicted V$NF-κB binding sites	
Matrix Family	p-value	Matrix Family	p-value
V$KLFS	1.038E-5	V$SP1F	1.67E-5
V$RXRF	2.11E-4	V$KLFS	8.61E-4
V$ETSF	0.019	V$ETSF	0.06
V$HAND	0.01	V$HAND	0.22

Table 3. Predicted TF-binding sites common to at least 86% of sequences Gene2Promoter program was used to search for transcription factor-binding sites common to at least 86% of sequences within 500bp upstream from the first TSS and 100bp downstream from the last TSS in proximal promoters. Input genes were those related to inflammatory process from both p65-alone and p65/p300 enriched genes. A more restrictive analysis was performed only in sequences with predicted V$NF-κB-binding sites. Sometimes the same gene with several TSS can be included. Raw data Weblink common TF-binding http://www.uv.es/eruizy/

have shown that p65 was bound to a higher number of genes related to cell proliferation compared to cell death or inflammation (Fig. 1D). Next, we studied whether one of these biological processes was overrepresented in p65/p300-target genes compared to total p65-bound genes. As shown in Fig. 4B, p65/p300 targets were more strongly enriched in a biological category included into the inflammatory response (Weblink to p65p300 and p65-alone inflammation raw data http://www.uv.es/eruizy/).

The result of this analysis suggests that p65/p300 represents a major complex preferentially involved in the modulation of the inflammatory response at 48h of mammary gland involution. Nevertheless, this suggestion does not rule out a dynamic gene expression regulation by NF-κB throughout the involution process. Although too extent for the present work, a deeper study of NF-κB-promoter binding during the time course of mammary gland involution, would provide further information on the dynamics of this transcription factor at each specific phase of mammary gland remodeling after pups withdrawal.

Cooperating elements in p65/p300 enriched promoters: Distance from TSS, density of NF-κB binding sites and other transcription factors

Studies on pro-inflammatory gene transcription have focused on proximal promoters for their closed proximity to TSS [32]. In order to define p65/p300-binding events in a more precise manner, we analyzed the number of correlations in our ChIP-on-Chip experiments versus the distance from transcriptional start sites. As shown in Fig. 5, we observed multiple p65-binding events scattered over upstream and downstream regions on gene promoters (-1000bp to +1000bp), with a mean number of correlations of 1075±377 Interestingly, p65/p300-binding showed a subpopulation specifically bound to a more restricted and narrower window located mainly at +139bp downstream from the TSS (mean of correlations of 328±175). This region has been recently suggested to have a lower nucleosome density in transcriptionally active genes [33]. This circumstance facilitates recruitment of the preinitiation complex and transcription factors to the TSS, leading to the transcription initiation. Therefore, our results might suggest that although p65 can bind to multiple sites on gene promoters or enhancers, most probably p300 accessibility is restricted to some particular p65 complexes bound near the TSS of genes. This fact would be responsible for the selection of specific gene transcription initiation.

However, transcriptional activation could require physical proximity to other transcription factors, either from the same or from a different matrix family. According to this model, NF-κB could synergistically activate transcription by a cooperative binding to DNA motifs present in tandem on gene promoters or enhancers.

To determine whether frequency of NF-κB-binding sites was involved in the specific selection of p65/p300-enriched genes during 48h mammary gland involution, we used the Gene2Promoter program to search for NF-κB

motifs. Frequency of NF-κB-binding sites was calculated as percentage of sequences with predicted binding sites at 500bp upstream from the first TSS and 100bp downstream from the last one. We used as input genes a selection of p65 alone- or p65/p300-enriched genes previously identified as part of the inflammatory process. Table 2 (Weblink to common TF-binding data http://www.uv.es/eruizy/) shows that both, p65 alone- and p65/p300-selected pro-inflammatory genes have predicted V$NF-κB-binding sites in at least 86% of sequences. Moreover, the analysis described above predicts that most of affected genes preferentially include a unique V$NF-κB-binding site at this region especially in the group of p65/p300-enriched group.

As mentioned, NF-κB transcriptional activity could also be mediated by cross-talk with transcription factors of different matrix families, resulting in either synergistic activation or antagonistic inhibition of gene expression [11]. Thus, we searched for transcription factor binding sites common to at least 86% of sequences for p65 alone- or p65/p300-enriched genes. We found multiple binding sites for both V$ETSF and V$KLFS in either p65-alone or p65/p300-enriched gene promoters (Table 3). In agreement with these results, a co-regulation of p65/NF-κB-controlled genes by Ets has been recently published [34].

Interestingly, when we restricted our analysis to only genes with predicted V$NF-κB-binding sites, we observed V$SP1F binding motifs common to at least 85% of sequences included in the p65/p300-group and absent from the p65-alone group. In this sense, it has been shown that for a number of gene promoters a functional interaction between NF-κB and Sp1 is required for full gene expression [35]. Furthermore, it is well known that selective regulation of genes by a transcription factor is highly dependent on chromatin structure. In this way, p65/p300 binding to some accessible sequences on gene promoters in the proximity of TSS would be enough for transcription initiation, although most probably a subset of genes would need further chromatin remodeling to remove nucleosome barriers. It has been demonstrated that nucleosomes are less stably assembled on CpG elements than on those low CpG promoters [36]. Therefore, in agreement with Ramirez-Carrozi et al, remodeling-independent transcriptional initiation would be favored in those genes such as p65/p300-enriched genes with a high prevalence of Sp1 binding sites, which are known to be GC-rich elements [37].

However, it is noteworthy to mention that our current understanding of the Sp1 binding sites, highlights the need for a deeper review. Indeed, the new models for the role of GC-sites on gene promoters emphasizes that these elements are not necessarily the target of Sp1, but instead can bind repressors and activators from the related matrix family V$KLFS (Krüpel-like zinc finger similar to Sp1). A group of KLF proteins represses transcription by recruitment of HDAC (histone deacetylase complex) through direct interaction with Sin3A [38]. Therefore, we do not rule out the possibility that the expression of those genes included into the p65-alone group could be repressed by some member of the KLF family of transcription factors which are over-represented in this group.

On the whole, although a more specific study on the role of these factors on NF-κB-inducible genes would be needed, it is tempting to speculate that the interplay between V$KLFS/V$SP1F and NF-κB could be responsible for the balance inclination to a particular biological process in mammary gland at 48h of involution.

Concluding Remarks

We have attempted to understand the selective regulation of NFκB-inducible genes included in a particular biological process during mammary gland involution. The diversity of mechanisms employed by NF-κB for transcriptional activation of inducible genes most probably reflects that each gene is subjected to a highly specific mode of regulation. Although taking into account this evident observation, identification of NF-κB-target genes is an essential step to elucidate the *in vivo* molecular profile of this important transcription factor. Moreover, NF-κB not only modulates cell death and proliferation, but it is also involved in tumor development and progression by the induction of an inflammatory environment [39] in some way similar to that one observed in the involuting mammary gland of mice. In fact, it has been suggested that deregulation of postlactational involution may act to facilitate tumor formation [40, 41]. Indeed, the elevated incidence of breast cancer associated with pregnancy has been suggested to be influenced by the tumor microenvironment developed in mammary gland after weaning [42]. In agreement with the tumor-promoting potential of the involuting mammary gland, we found that 81% of p65/p300-enriched genes passing the disease filter (MeSH), fell into the category of neoplasm. Therefore, the availability of a set of NF-κB-target genes during mammary gland involution will represent an

important instrument for further studies on both, the role of these genes in breast cancer, as well as the development of putative prognosis markers or new therapeutical targets. Finally, our analysis opens a wide window for new approaches and future investigation on the molecular mechanisms of NF-κB gene selection.

Acknowledgements

This work was supported in part by grants from Plan Nacional I+D+I (BFU2010-18253) and Generalitat Valenciana (PROMETEO 2010-075) to J.R.V. and Ministerio de Ciencia e Innovación (FIS PS09-02360) to E.R.G-T. A.B. is a fellow from Ministerio de Ciencia e Innovación (programa Rio Hortega).

References

1 Lund LR, Romer J, Thomasset N, Solberg H, Pyke C, Bissell MJ, Danø K, Werb Z: Two distinct phases of apoptosis in mammary gland involution: proteinase-independent and -dependent pathways. Development 1996;122:181-193.

2 Wiesen J, Werb Z: Proteinases, cell cycle regulation, and apoptosis during mammary gland involution. Mol Reprod Dev 2000;56:534-540.

3 Zaragozá R, Miralles VJ, Rus AD, García C, Carmena R, García-Trevijano ER, Barber T, Pallardó FV, Torres L, Viña JR: Weaning induces NOS-2 expression through NF-κB modulation in the lactating mammary gland: importance of GSH. Biochem J 2005;391:581-588.

4 Zaragozá R, Bosch A, García C, Sandoval J, Serna E, Torres L, García-Trevijano ER, Viña JR: Nitric oxide triggers mammary gland involution after weaning: remodelling is delayed but not impaired in mice lacking inducible nitric oxide synthase. Biochem J 2010;428:451-462.

5 Stein T, Morris JS, Davies CR, Weber-Hall SJ, Duffy M-A, Heath VJ, Bell AK, Ferrier RK, Sandilands GP, Gusterson BA: Involution of the mouse mammary gland is associated with an immune cascade and an acute-phase response, involving LBP, CD14 and STAT3. Breast Cancer Res 2004;6:R75-R91

6 Clarkson RW, Wayland MT, Lee J, Freeman T, Watson CJ: Gene expression profiling of mammary gland development reveals putative roles for death receptors and immune mediators in post-lactational regression. Breast Cancer Res 2004;6:R92-109.

7 Aggarwal BB, Kunnumakkara AB, Harikumar KB, Gupta SR, Tharakan ST, Koca C, Dey S, Sung B: Signal transducer and activator of transcription-3, inflammation, and cancer: how intimate is the relationship? Ann N Y Acad Sci 2009;1171:59-76.

8 Shaulian E: AP-1—The Jun proteins: Oncogenes or tumor suppressors in disguise? Cell Signal 2010;22:894-899.

9 Reuter S, Gupta SC, Chaturvedi MM, Aggarwal BB: Oxidative stress, inflammation, and cancer: how are they linked? Free Radic Biol Med 2010;49:1603-1616.

10 Baud V, Karin M: Is NF-kappaB a good target for cancer therapy? Hopes and pitfalls. Nat Rev Drug Discov 2009;8:33-40.

11 Perkins ND: Integrating cell-signalling pathways with NF-kappaB and IKK function. Nat Rev Mol Cell Biol 2007;8:49-62.

12 Brantley DM, Yull FE, Muraoka RS, Hicks DJ, Cook CM, Kerr LD: Dynamic expression and activity of NF-kappaB during post-natal mammary gland morphogenesis. Mech Dev 2000;97:149-155.

13 Clarkson RW, Heeley JL, Chapman R, Aillet F, Hay RT, Wyllie A, Watson CJ: NF-kappaB inhibits apoptosis in murine mammary epithelia. J Biol Chem 2000;275:12737-12742.

14 Cao Y, Bonizzi G, Seagroves TN, Greten FR, Johnson R, Schmidt EV, Karin M: IKKalpha provides an essential link between RANK signaling and cyclin D1 expression during mammary gland development. Cell 2001;107:763-775.

15 Romieu-Mourez R, Kim DW, Shin SM, Demicco EG, Landesman-Bollag E, Seldin DC, Cardiff RD, Sonenshein GE: Mouse mammary tumor virus c-rel transgenic mice develop mammary tumors. Mol Cell Biol 2003;16:5738-5754.

16 Brantley DM, Chen CL, Muraoka RS, Bushdid PB, Bradberry JL, Kittrell F, Medina D, Matrisian LM, Kerr LD, Yull FE: Nuclear factor-kappaB (NF-kappaB) regulates proliferation and branching in mouse mammary epithelium. Mol Biol Cell 2001;12:1445-1455.

17 Zhou Y, Eppenberger-Castori S, Eppenberger U, Benz CC: The NF-kappaB pathway and endocrine-resistant breast cancer. Endocr Relat Cancer 2005;12 Suppl 1:S37-46.

18 Fan Y, Dutta J, Gupta N, Fan G, Gélinas C: Regulation of programmed cell death by NF-kappaB and its role in tumorigenesis and therapy. Adv Exp Med Biol 2008;615:223-250.

19 Connelly L, Barham W, Pigg R, Saint-Jean L, Sherrill T, Cheng DS, Chodosh LA, Blackwell TS, Yull FE: Activation of nuclear factor kappa B in mammary epithelium promotes milk loss during mammary development and infection. J Cell Physiol 2010;222:73-81.

20 Torres L, Sandoval J, Penella E, Zaragozá R, García C, Rodríguez JL, Viña JR, García-Trevijano ER: In vivo GSH depletion induces c-myc expression by modulation of chromatin protein complexes. Free Radic Biol Med 2009;46:1534-1542.

21 Tusher VG, Tibshirani R, Chu G: Significance analysis of microarrays applied to the ionizing radiation response. Proc Natl Acad Sci USA 2001;98:5116-5121.

22 Kirillova I, Chaisson M, Fausto N: Tumor necrosis factor induces DNA replication in hepatic cells through nuclear factor kappaB activation. Cell Growth Differ 1999;10:819-828.

23 Bourgarel-Rey V, Vallee S, Rimet O, Champion S, Braguer D, Desobry A, Briand C, Barra Y: Involvement of nuclear factor kappaB in c-Myc induction by tubulin polymerization inhibitors. Mol Pharmacol 2001;59:1165-1170.

24 Farnham P: JInsights from genomic profiling of transcription factors. Nat Rev Genet 2009;10:605-616.

25 Zaragozá R, Torres L, García C, Eroles P, Corrales F, Bosch A, Lluch A, García-Trevijano ER, Viña JR: Nitration of cathepsin D enhances its proteolytic activity during mammary gland remodelling after lactation. Biochem J 2009;419:279-288.
26 Teferedegne B, Green MR, Guo Z, Boss JM: Mechanism of action of a distal NF-kappaB-dependent enhancer. Mol Cell Biol 2006;26:5759-5770.
27 Calao M, Burny A, Quivy V, Dekonink A, Van Lint C: A pervasive role of histone acetyltransferase and deacetylases in NF-κB-signaling code. Trends Biochem Sci 2008;33:339-349.
28 Vo N, Goodman RH: CREB-binding protein and p300 in transcriptional regulation. J Biol Chem 2001;276:13505-13508.
29 Sandoval J, Rodríguez JL, Tur G, Serviddio G, Pereda J, Boukaba A, Sastre J, Torres L, Franco L, López-Rodas G: GRNAPol-ChIP: a novel application of chromatin immunoprecipitation to the analysis of real-time gene transcription. Nucleic Acids Res 2004;32:e88.
30 Ito K, Barnes PJ, Adcock IM: Glucocorticoid receptor recruitment of histone deacetylase 2 inhibits interleukin-1beta-induced histone H4 acetylation on lysines 8 and 12. Mol Cell Biol 2000;20:6891-6903.
31 Guenther MG, Levine SS, Boyer LA, Jaenisch R, Young RA: A chromatin landmark and transcription initiation at most promoters in human cells. Cell 2007;130:77-88.
32 Smale ST: Selective transcription in response to an inflammatory stimulus. Cell 2010;140:833-844.
33 Bai L, Morozov AV: Gene regulation by nucleosome positioning. Trends Genet 2010;26:476-483.
34 De Siervi A, De Luca P, Moiola C, Gueron G, Tongbai, Chandramouli GV, Haggerty C, Dzekunova I, Petersen D, Kawasaki E, Kil WJ, Camphausen K, Longo D, Gardner K: Identification of new Rel/NFkappaB regulatory networks by focused genome location analysis. Cell Cycle 2009;8:2093-2100.
35 Hirano F, Tanaka H, Hirano Y, Hiramoto M, Handa H, Makino I, Scheidereit C: Functional interference of Sp1 and NF-κB through the same DNA binding site. Mol Cell Biol 1998;18:1266-1274.
36 Segal E, Fondufe-Mittendorf Y, Chen L, Thåström A, Field Y, Moore IK, Wang JP, Widom J: A genomic code for nucleosome positioning. Nature 2006;442:772-778.
37 Ramirez-Carrozzi VR, Braas D, Bhatt DM, Cheng CS, Hong C, Doty KR, Black JC, Hoffmann A, Carey M, Smale ST: A unifying model for the selective regulation of inducible transcription by CpG islands and nucleosome remodeling. Cell 2009;138:114-128.
38 Lomberk G, Urrutia R: The family feud: turning off Sp1 by Sp1-like KLF proteins. Biochem J 2005;392:1-11
39 Chariot A: The NF-kappaB-independent functions of IKK subunits in immunity and cancer. Trends Cell Biol 2009;19:404-413.
40 Radisky DC, Hartmann LC: Mammary involution and breast cancer risk: transgenic models and clinical studies. J Mammary Gland Biol Neoplasia 2009;14:181-191.
41 Schedin P, O'Brien J, Rudolph M, Stein T, Borges V: Microenvironment of the involuting mammary gland mediates mammary cancer progression. J Mammary Gland Biol Neoplasia 2007;12:71-82.
42 Lyons TR, O'Brien J, Borges VF, Conklin MW, Keely PJ, Eliceiri KW, Marusyk A, Tan AC, Schedin P: Postpartum mammary gland involution drives progression of ductal carcinoma in situ through collagen and COX-2. Nat Med 2011;17:1109-11015.